**NASA DEVELOP National Program**
**Colorado – Fort Collins**
*Spring 2022*

# Boulder County Disasters

## Mapping Forest Carbon Stocks to Understand Carbon Implications of Treatment and Wildfire

**DEVELOP Technical Report**
Final – April 2nd, 2022

Sarah Hettema (Project Lead)
Jennifer Rogers
Ibuki Sugiura
Erin Twaddell

***Advisors:***
Dr. Anthony Vorster, Colorado State University, Natural Resource Ecology Laboratory (Science Advisor)
Nicholas Young, Colorado State University, Natural Resource Ecology Laboratory (Science Advisor)
Peder Engelstad, Colorado State University, Natural Resource Ecology Laboratory (Science Advisor)
Dr. Paul Evangelista, Colorado State University, Natural Resource Ecology Laboratory (Science Advisor)
Dr. Catherine Jarnevich, USGS, Fort Collins Science Center (Science Advisor)

# 1. Abstract

In recent years, record-breaking wildfire activities in the western US illustrate the need for fire mitigation efforts, such as forest fuels reduction treatments. Forests serve as crucial carbon sinks that combat the increasing effects of climate change while fuels reduction treatments may remove carbon from forested systems. As a result, forest managers need to find a balance between fire mitigation and carbon preservation. This project partnered with Boulder County Parks and Open Space (BCPOS) and the University of Colorado, Denver to investigate the 2020 Cal-Wood fire in Boulder County, Colorado. Using remote sensing data from Landsat 8 OLI, SRTM, Sentinel-2 MSI, and LiDAR, we mapped post-fire forest carbon pools and compared these values with values derived from measurements from plots on the ground. Results indicate that the correlations are $R^2$=0.76 for aboveground live carbon, $R^2$=0.44 for standing carbon, and $R^2$=0.43 for aboveground dead carbon (R2=0.43), and $R^2$=0.35 for total carbon (R2=0.35). Additionally, 38.5% of total carbon was stored in dead carbon and 14.4% was stored in live carbon. We next compared the post-fire pools between treated and untreated areas. Our analysis suggests fuels reduction treatments did not reduce carbon loss in the presence of wildfire enough to clearly distinguish the post-fire carbon in the treated and untreated areas. However, our final carbon maps still provide BCPOS and researchers with an opportunity to explore carbon estimation models based on remotely sensed data as well as a framework to evaluate fuels reduction treatment effectiveness and impact on forest carbon stocks for future wildfire events.

**Key Terms**
random forests, remote sensing, LiDAR, forest management, wildfire, carbon

# 2. Introduction

## *2.1 Background Information*

In recent decades, western US forests have experienced multiple wildfire events accompanied by record-breaking area burned, frequency, and fire-season length (Abatzoglou & Williams, 2016). This increased trend in record-breaking wildfire events coincides with climatic conditions more conducive to wildfire and is exacerbated by a history of fire suppression (Abatzoglou & Williams, 2016; Agee & Skinner, 2005). Due to these trends, land managers are now considering forest carbon preservation in their policies in an attempt to mitigate both wildfire severity and climate change (Dilling et al., 2016). Thinning and prescribed burns are common fuels reduction treatments to reduce fuel accumulation, fuel continuity, and the associated risk of high-severity fire (Campbell et al., 2012). These treatments serve to temporarily reduce wildfire hazards and may also serve other management objectives, including native species restoration, increased biodiversity, and increased terrestrial carbon storage (Campbell et al., 2012). However, considering that forests sequester carbon in above and below ground biomass, any disturbance event, such as fuels reduction treatments, will redistribute forest carbon stocks into different forms (e.g., ash, dead biomass, atmospheric $CO_2$) (Vashum and Jayakumar, 2012).

One strategy for climate change mitigation is to preserve the carbon pools on the ground and minimize release of $CO_2$ to the atmosphere. In this context, $CO_2$ release associated with fuels reduction treatments can be considered as an upfront cost to mitigate larger $CO_2$ release through more severe fires in the absence of such

treatments (Dilling et al., 2016). Therefore, it is important to investigate the effects of fuels reduction treatments on wildfire-induced carbon loss to understand how western US forest carbon stocks are responding to management efforts and wildfire under changing climate conditions. In the state of Colorado (CO), these trends in record-breaking fire events have rendered many Wildland Urban Interfaces (WUI) at risk, thus prompting fuels reduction treatments in surrounding forests (Liu et al., 2015). Our project considered some of the heavily managed forests along the CO Front Range WUI and built upon previous DEVELOP projects (see section 2.1.1) to explore the impacts of fuels reduction treatments and the 2020 Cal-Wood fire on post-fire carbon stocks.

### *2.1.1 Relevant Work*

In Spring 2021, the CO Front Range Disasters DEVELOP team produced research considering the broader perspective of forest management on the Cameron Peak and Cal-Wood fires (Swayze et al., 2021). They utilized Landsat 8 remote sensing imagery to assess the relationship between burn severity, environmental and topographic variables, and fuels reduction treatments. The project associated thinning and prescribed fire treatment variations with a higher detected burn severity, while Wildfire and Prescribed Burn & Wildfire treatments were associated with lower detected burn severity. Though the results from this study aligned with wildfire management objectives, they did not consider broader carbon management objectives (Swayze et al., 2021). We utilized the produced burn severity map and consolidated forest treatment data to inform our partners of the impact of wildfire severity and fuels reduction treatments on subsequent carbon loss.

The combination of remote sensing technology with ground-truthed data is a growing field of study, though more work needs to be done to understand the full capability of this research (Tsitsi, 2016). As the Fall 2020 Fischer's Peak Ecological Forecasting DEVELOP team explored the feasibility of combining remote sensing and ground-truthed data with the machine-learning method of random forest (RF) to estimate landscape-scale biomass. RF uses iterative decision trees to estimate the importance of variables while avoiding overfitting and is often used in ecological modeling (Biau & Scornet, 2016; Genuer et al., 2010). In this project, we assessed the feasibility of estimating carbon stocks using a similar approach.

### *2.1.2 Project Partners & Objectives*

The partners for this project included land managers for Boulder County Parks and Open Space (BCPOS), the City of Boulder, and Jefferson County, as well as researchers at the University of Colorado, Denver. The objectives of this study were to 1) train carbon estimation models with forest inventory field plot data derived from the City of Boulder and Jefferson County, then simulate post-wildfire carbon for Boulder County using satellite imagery, high-resolution light detection and ranging (LiDAR) data, and other sources, and 2) utilize models to map post-wildfire forest carbon in order to estimate the effects of wildfire events and fuels reduction treatments on carbon preservation. The final forest carbon maps, treatment evaluations between post-wildfire treated and untreated stands, and an Esri StoryMap that communicates these findings to stakeholders and the public were provided to BCPOS to refine future treatment strategies.

## ***2.2 Study Area***

The CO Front Range represents the junction between the Rocky Mountains and the Great Plains. This region includes a range of vegetation zones due to varying topographic and climatic factors (Addington et al., 2018). The eastern slopes of this region are known for dry winds of speeds greater than 162 km/hr, increasing the desiccation of the landscape and thus spreading fire (Veblen & Lorenz, 1991). This study focuses on the moisture-limited montane zone (1,500 to 2,830 m) from the Heil Valley Ranch Property in Boulder County south to White Ranch Park in Jefferson County. The lower montane is dominated by a dry coniferous forest type, primarily composed of ponderosa pine (*Pinus ponderosa*) (Addington et al. 2018). Historic fire return intervals of ca. 10-30 years on average in the lower montane limited fuel continuity, which allowed for a relatively mixed-severity fire regime in these systems (Kaufmann et al., 2006). Due to a history of wildfire suppression, these forests have developed productive understories of grasses, shrubs, and shade-tolerant tree species (e.g., Douglas-fir (*Pseudotsuga mensiesii*) and Rocky Mountain juniper (*Juniperus scopulorum*)), allowing for the accumulation of fuels. Changing climatic factors, such as warming temperatures, dry summers, and below-average winter precipitation (Westerling, 2016), increase the drying conditions that lengthen the wildfire season. Thus, land managers from BCPOS, the City of Boulder, and Jefferson County have employed thinning and prescribed burning treatments on these forests to moderate subsequent wildfire behavior.

### *2.2.1 The Cal-Wood Fire*

The 2020 Cal-Wood fire started on October 17th and consumed over 10,000 acres of highly managed forests of the Heil Valley Ranch property in Boulder County (Figure 1), thus presenting the unique opportunity to understand how fuels reduction treatments, wildfire, and carbon interact. In five hours, a total of 5,000 acres were burned, and after 24 hours, the fire had burned almost 9,000 acres. The fire coincided with very dry conditions and nearby winds of 50 miles per hour (B. Buma & N. Stremel, personal communication, 2020).

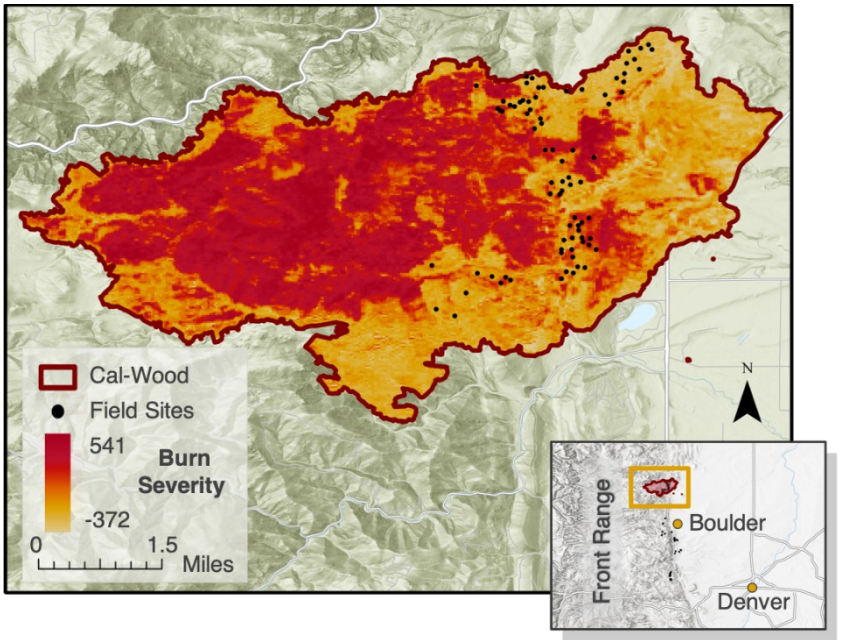


*Figure 1.* Study area map highlighting the perimeter and burn severity (unitless) of the 2020 Cal-Wood fire as well as the locations of the Summer 2021 field plots

throughout Heil Valley Ranch. The inset provides locational context of the Cal-Wood fire in relation to Boulder, CO and Denver, CO.

# 3. Methodology

## *3.1 Data Acquisition*

In order to launch this project, the University of Colorado, Denver collected biomass and carbon plot-level data in the summer of 2021 in Jefferson County, Boulder County, and the City of Boulder. The 130 20m$^2$ plots were all located within ponderosa pine forests and were roughly the same elevation. Of these, 80 were within the Cal-Wood wildfire perimeter. Colorado State University (CSU) provided us with an updated burn severity raster that encompasses the Cal-Wood fire perimeter. Burn severity represents the differenced normalized burn ratio (dNBR) ranging from -372 to 541 in our study area, indicating high-levels of enhanced vegetation regrowth to moderately high-severity burns (Key & Benson, 2006). We gathered treatment data from a joint Treatment Database maintained by CSU, Colorado Forest Restoration Institute, BCPOS, NASA DEVELOP, and Colorado State Forest Service. The treatment data included the location, type, and date of treatments that occurred in the region. We downloaded existing vegetation type and forest canopy cover data from the national LANDFIRE program website. The Natural Resource Ecology Laboratory at CSU also provided us with the fire perimeter data that was used as a boundary for our model. We additionally procured data from the Natural Resources Conservation Service (NRCS) Web Soil Survey for soil characteristics as well as Oak Ridge National Laboratory's (ORNL) Distributed Active Archive Center (DAAC) soil carbon estimates.

In addition, we accessed and gathered satellite imagery from Landsat 8 Operational Land Imager (OLI) tier 1 Top of Atmosphere (TOA) and Sentinel-2 Multispectral Imager (MSI) Level-1C through Google Earth Engine (GEE), as well as preprocessed Shuttle Radar Topography Mission (SRTM) incorporated into the USGS's National Elevation Dataset (NED). We were also provided with 30m$^2$ resolution gridded 2013 LiDAR data from the Vogeler Research Lab at CSU in order to incorporate canopy height metrics. A comprehensive list of all the predictor variables that we considered in our model can be found in Table A1. A comprehensive workflow is summarized in Figure 2.

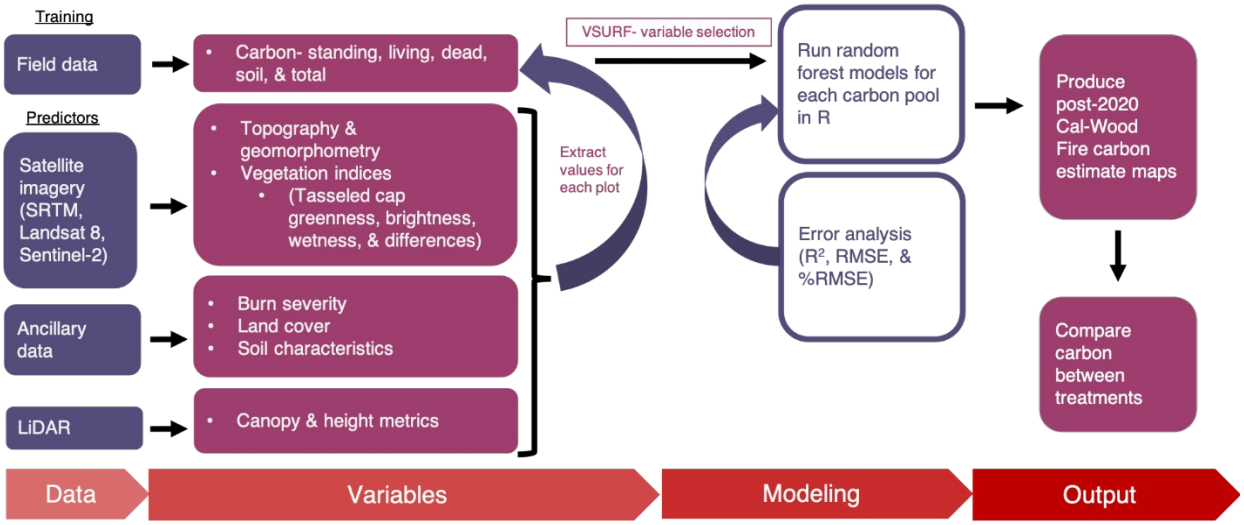


*Figure 2.* Flow chart outlining general methodological flow.

We converted aboveground biomass estimates to carbon at a pre-established 2-to-1 ratio by dry weight (Penman et al., 2003; Rebain, 2010). We characterized the carbon plot data into five major carbon pools, including standing, aboveground live, aboveground dead, soil, and total carbon. Standing carbon included both living and dead trees. Aboveground live carbon included living trees, saplings, shrubs, and grasses. Aboveground dead carbon included dead trees, seedlings, shrubs, and woody debris. Soil carbon included both organic and mineral soils. Total carbon included aboveground live, aboveground dead, and soil carbon collectively. Aside from the total carbon pool, the standing pool had the largest measure of carbon in a given plot, while the living had the smallest (Table 1). Preliminary results acquired by our partners at the University of Colorado, Denver suggest wildfire carbon losses were not offset by the carbon removed through treatments. To explore these results at a continuous spatial scale, we first used these carbon data to provide ground-truthed estimates for our training and validation datasets. For our models, the treatment type for each plot was further categorized into Thin, Thin & Prescribed Burn (Rx Burn), Wildfire (the 2003 Overland wildfire), and No Treatment. Treatment age was considered to be the difference between 2020 and the year of the most recent treatment. A third variable, treatment presence, simply indicates whether a plot was treated or not.

*Table 1.* Summary statistics of the different carbon pools of the 80 field plots contained within the Cal-Wood fire perimeter used as training data.

| Carbon Pool | Maximum (Mg/ha) | Minimum (Mg/ha) | Median (Mg/ha) | Mean (Mg/ha) | Std. Dev. (Mg/ha) |
|---|---|---|---|---|---|
| Standing Carbon | 113.59 | 0.00 | 35.05 | 35.64 | 26.11 |
| Aboveground Live Carbon | 77.81 | 0.11 | 1.82 | 13.95 | 22.09 |
| Aboveground Dead Carbon | 113.59 | 0.00 | 18.16 | 25.67 | 28.02 |
| Soil Carbon | 94.03 | 20.77 | 42.85 | 44.99 | 14.02 |
| Total Carbon | 155.90 | 26.42 | 85.09 | 84.61 | 30.79 |

### *3.2 Data Processing*

#### *3.2.1 Data*

In GEE, we filtered Landsat 8 images to only include imagery with less than 0.5% cloud cover. Due to limited imagery for this time period, Sentinel-2 was limited to imagery with less than 3.5% cloud cover. From the filtered collection, we selected images of a date before the fire and three after the fire (Fall, Spring, and Summer). We resampled Sentinel-2 imagery to 30m resolution to match Landsat 8. From these images, we computed three tasseled cap transformations: brightness, greenness, and wetness. This was done by weighing the bands, or multiplying wavelengths, by empirically established coefficients specific to our sensors (Tables B1 & B2) (Baig et al., 2014; Shi & Xu 2019). Tasseled cap indices are often used in ecological studies for their ability to distinguish the landscape on a spectrum of vegetation density, vegetation moisture, and soil moisture and to characterize certain landscapes such as water or concrete (Ali & Salman, 2016). We also computed the difference between Summer pre-fire and Spring post-fire tasseled cap indices to represent changes attributable to the fire, as well as the difference between Spring and Summer post-fire tasseled cap indices to represent vegetation regrowth. All indices and differences were then exported from GEE and input into RStudio (R). We derived slope, aspect, northness, eastness, curvature, plan curvature, profile curvature, heat load index, roughness, and compound topographic index (CTI) layers from the NED using the ArcGIS Geomorphometry & Gradient Metrics Toolbox (Evans et al., 2014). We also incorporated areal LiDAR height and canopy metrics (Table A1).

#### *3.2.2 Model Development*

After importing our layers into R, we converted them to the same geographic coordinate system (unprojected WGS84), resampled using a Landsat 8 image to achieve the same cell sizes, and then cropped them all to the Cal-Wood fire perimeter. We then stacked the raster layers and extracted the values for each field plot. We compared extracting values both at the pixel-level and as the mean value including the four adjacent pixels. After not observing any distinction in the model's performance, we proceeded at the pixel-level for ease. Additionally, we explored running models using all 130 field plots; this resulted in poorer performing models and, due to our interest in mapping burned areas, we proceeded with the 80 contained in the fire. In order to narrow down our variable selection to create models that did not overfit, using roughly $1/10^{th}$ the number of predictor variables to data points, we used the R package Variable Selection Using Random Forests (VSURF) to select the best performing predictor variables (Harrell et al., 1996). By iteratively assessing variable importance and error, VSURF assists in eliminating irrelevant and redundant variables while selecting those best for model predictability. We manually removed highly correlated variables ($>|\pm 0.7|$) when VSURF selected greater than our ideal number of variables (i.e., 8).

We then used the subset of VSURF-derived variables to train a RF supervised machine learning algorithm model using the randomForest package in R. For all RF model runs, we used 1000 decision trees and 1 to 3 variables at each node. The best number of variables to split into at each node, offering the most accuracy, was chosen by running various iterations while seeking to minimize model error. The number of decision trees was determined by comparing the number of trees to the mean-squared error.

Two RF model types were investigated for our response variables, the amount of carbon in each pool: 1) a model where VSURF was presented with all the predictor variables excluding treatment data, such as treatment types, age, and presence (Non-Treatment Model) and 2) a model where VSURF was presented with all predictor variables, including those three treatment variables (Treatment Model). Our main model (Non-Treatment Model) did not consider treatment information because it would bias future analyses of treatment effects on carbon preservation. However, including treatment data altered the predictor variables selected by VSURF and improved model accuracy for some carbon pools (Table C1). Thus, we considered Treatment Models separate from Non-Treatment Models. We calculated model performance as the coefficient of determination ($R^2$), Root Mean Square Error (RMSE), and Percent Root Mean Square Error (RMSE/Mean or %RMSE) from the predicted versus observed outputs for carbon. Once our best Non-Treatment Models were selected (Table 2), a raster stack of all the predictor layers was input into the raster predict function to develop a map estimating carbon on the landscape.

# 4. Results & Discussion

## *4.1 Analysis of Results*

### *4.1.1 Non-Treatment Model Outcomes*

The $R^2$ value, a measure of model accuracy, was the greatest for the aboveground live carbon pool model (0.76), followed by 0.44 for the standing carbon pool, 0.43 for the aboveground dead carbon pool model, and 0.35 for the total carbon pool (Table 2). The model for the soil carbon pool, which can be difficult to estimate from aboveground proxies, had the smallest $R^2$ value of 0.13. The total carbon pool had one of the smallest %RMSE (29.2%), while the aboveground live (77.8%) and dead carbon (81.5%) pool models demonstrated large discrepancies from the field-derived data.

*Table 2*. List of best models and their performance ratings for each Non-Treatment carbon pool model.

| Carbon Pool | $R^2$ | RMSE (Mg/ha) | %RMSE | Predictor Variables (in order of importance) |
|---|---|---|---|---|
| Aboveground Live Carbon | 0.76 | 10.8 | 77.8% | • Post-fire tasseled cap greenness (Fall 2020)<br>• Burn severity<br>• Regrowth-related difference in tasseled cap brightness |
| Standing Carbon | 0.44 | 19.5 | 54.6% | • Forest canopy cover<br>• Average LiDAR canopy height<br>• Pre-fire tasseled cap wetness |
| Aboveground Dead Carbon | 0.43 | 20.9 | 81.5% | • Fire-related difference in tasseled cap greenness<br>• Post-fire tasseled cap greenness (Spring 2021) |

| | | | | |
|---|---|---|---|---|
| | | | | • Elevation |
| Total Carbon | 0.35 | 24.7 | 29.2% | • Average LiDAR canopy height<br>• Post-fire tasseled cap brightness (Spring 2021)<br>• Post-fire tasseled cap greenness (Fall 2020) |
| Soil Carbon | 0.13 | 13.0 | 28.9% | • Post-fire tasseled cap wetness (Fall 2020)<br>• Post-fire tasseled cap greenness (Fall 2020)<br>• Heat load index |

### *4.1.2 Treatment Model Outcomes*

When presented as options to VSURF, Treatment Models for aboveground dead, total carbon, and soil carbon incorporated one or more of the three treatment variables (presence, type, and age), whereas aboveground live and standing carbon did not. Specifically, the aboveground dead model incorporated all three, whereas total carbon incorporated treatment type and age, and soil carbon just treatment type. For soil carbon, treatment type became the most important predictor variable. This caused a notable improvement in model performance for both the total carbon and soil carbon models (Table C1). The $R^2$ for total carbon increased from 0.35 to 0.40 and soil carbon increased from 0.13 to 0.20. These statistics suggest that the inclusion of treatment information in some instances has the potential to improve carbon models.

### *4.1.3 Non-Treatment Model Evaluation and Estimated Carbon Maps*

We focused our modeling efforts on aboveground carbon pools due to the inherent difficulty of utilizing remote sensing technology to estimate belowground carbon (i.e., soil carbon). After reviewing $R^2$ and %RMSE values, we specifically selected three carbon pools for further analysis: aboveground live, aboveground dead, and total carbon.

#### *4.1.3.1 Aboveground Live Carbon Pool*

The three most important predictor variables, out of eight, for the aboveground live carbon pool model were post-fire tasseled cap greenness for Fall 2020, burn severity, and post-fire regrowth-related difference in tasseled cap brightness. In areas near the perimeter of the Cal-Wood fire burn perimeter, where burn severity was generally lower, there was a relatively higher volume of carbon, with the highest value being 65 Mg/ha (Figure 3a). The comparison between the model's estimated and field-derived plot-level carbon data illustrated that the model may underestimate live carbon values (Figure 3b). Additionally, the point at which the predicted measurements reach their maximum value was often its saturation point, which is a limitation of optical sensing for biomass. This is apparent in the actual measurements as they exceed this value (Figure 3b).

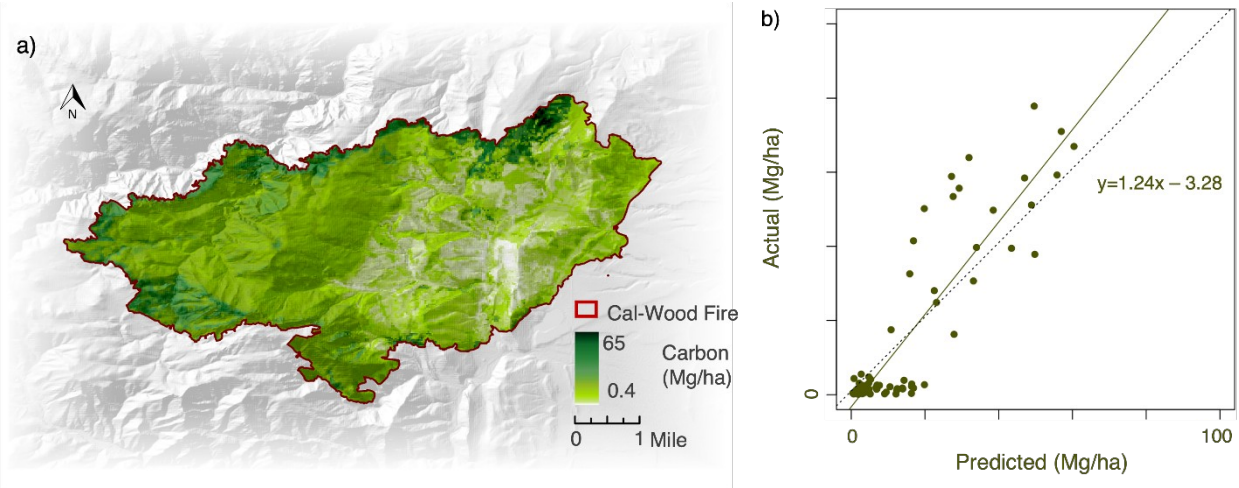


*Figure 3. a)* Estimated aboveground live carbon map. *b)* Comparison between the model estimates and field-derived carbon data. The dotted line represents a one-to-one relationship indicating a perfect model, and the solid green line represents the linear relationship between actual and predicted carbon values.

### *4.1.3.2 Aboveground Dead Carbon Pool*

For the aboveground dead carbon pool model, we found that fire-related difference in tasseled cap greenness, post-fire tasseled cap greenness for Spring 2021, and elevation were the top three predictor variables out of eight. Most of the carbon within the burn perimeter of this high-severity wildfire seemed to be stored as aboveground dead carbon, with a maximum of 129 Mg/ha (Figure 4a). The estimated and actual carbon stocks aligned reasonably well, with the model tending to slightly underestimate (Figure 4b).

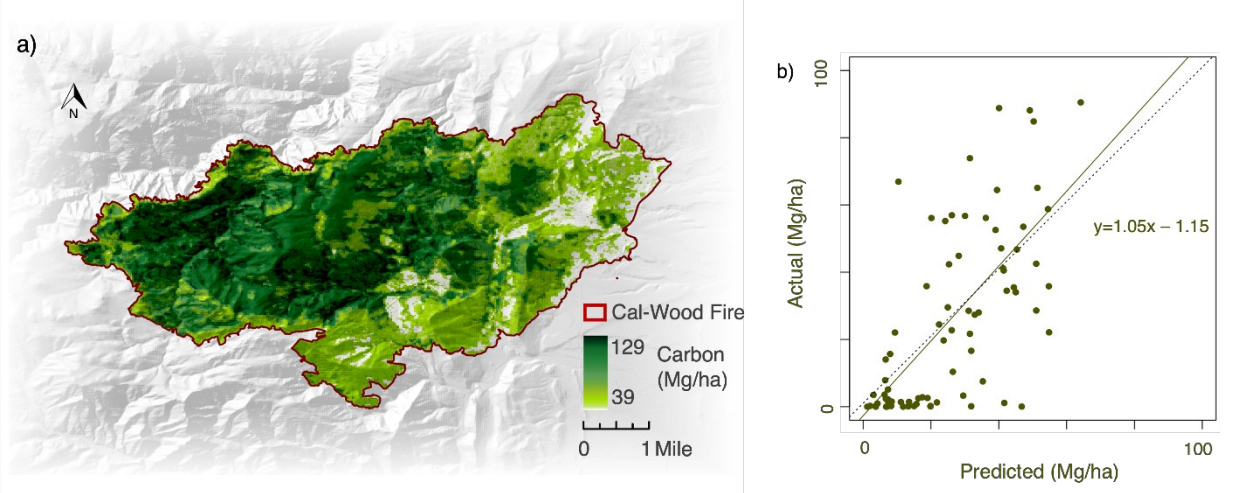


*Figure 4. a)* Estimated aboveground dead carbon map. *b)* Comparison between the model estimates and field-derived carbon data.

### *4.1.3.3 Total Carbon Pool*

Among five predictor variables, average LiDAR-derived canopy height, post-fire tasseled cap brightness for Spring 2021 and post-fire tasseled cap greenness for Fall 2020 were the three most important predictor variables for the total carbon pool model. The carbon distribution in the estimated total carbon pool was similar

to that of the dead carbon pool but showed slightly higher overall carbon values (maximum of 136 Mg/ha; Figure 5a). In addition, the estimated and actual carbon stocks aligned reasonably well (Figure 5b).

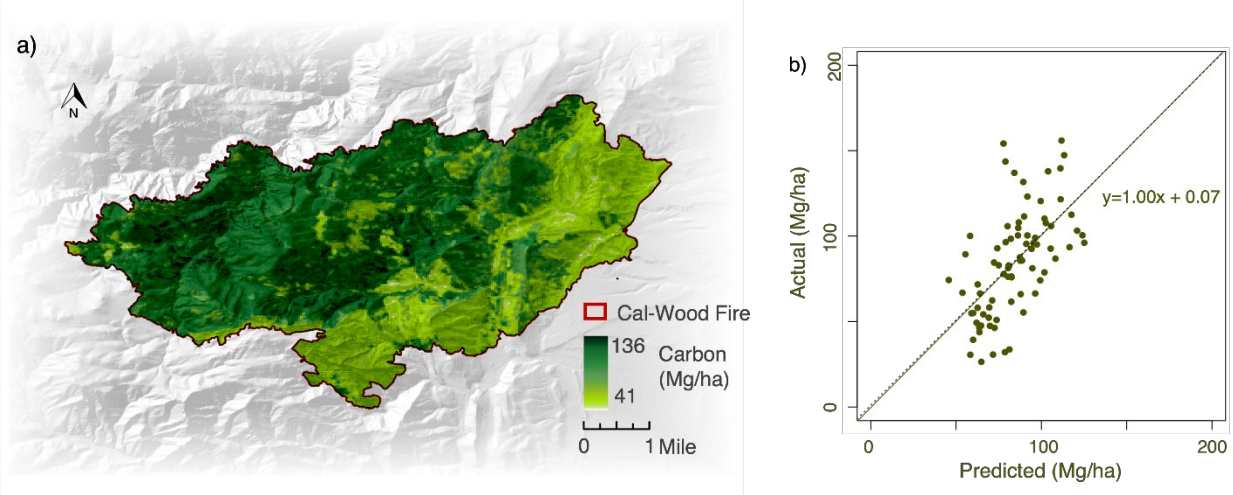


*Figure 5. a)* Estimated total carbon map. *b)* Comparison between the model estimates and field-derived carbon data.

### *4.1.4 Comparison of Aboveground Live, Aboveground Dead, and Total Carbon Pools (Non-Treatment Models)*

Before estimating the potential effect of treatment on forest carbon preservation, we first removed areas that were unforested, areas with minimal treatment records, and areas that buffered our treatment areas in order to not bias our results. Our models estimated ~600 Gg of aboveground live carbon, ~1600 Gg of aboveground dead carbon, and ~4100 Gg of total carbon within the burn perimeter. The aboveground dead carbon pool, accounting for 38.5% of the estimated total carbon, was greater in size than the aboveground live carbon pool, which only accounted for 14.4% of total carbon (Figure 6). The high discrepancy in carbon between the dead and live carbon pools illustrated a substantial carbon loss due to the fire. Approximately 53% of the simulated total carbon pool belonged to aboveground carbon, both live and dead. The remaining total carbon can be attributed to soil carbon and errors inherent in our models. This agrees with the field plot data, as on average, roughly half of the total carbon consisted of soil carbon (Table 1).

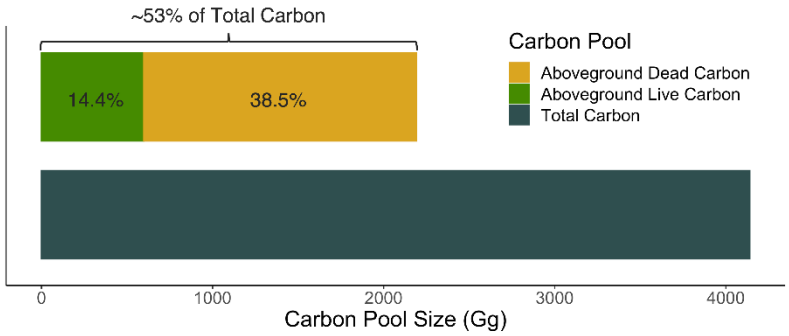

*Figure 6.* Comparison of the carbon pool size (Gg) where aboveground dead carbon is depicted in yellow, aboveground live carbon in green, and total carbon in navy blue.

### *4.1.5 Interaction with Treatment Variables (Non-Treatment Models)*

Based on the predicted aboveground live carbon map, we observed that Wildfire (12.4 Mg/ha), Untreated (12.3 Mg/ha), and Thin and Rx Burn (9.89 Mg/ha) treatments had the largest median values of aboveground live carbon (Figure 7a). Preforming a pairwise Wilcoxon rank sum test using a significance threshold of $p<0.01$ offered additional insights. Specifically, we noted that Thin & Rx Burn was significantly different from Wildfire and overall, the top three treatment types were statistically different from the bottom four. However, we did observe that most treatments varied in their effect on carbon (Figure 7a). Moreover, dead carbon exhibited a similar trend, with Untreated areas preserving higher amounts of carbon, as seen by its median value (46.3 Mg/ha), followed by Thin (36.5 Mg/ha), and Thin Twice (23.6 Mg/ha) (Figure 7b). For the aboveground dead carbon pool, most treatments were statistically different in their effects on carbon, aside from Rx Burn and Wildfire & Thin as well as Thin & Rx Burn and Wildfire (Figure 7b). Here, it may be important to consider that treatments with low values of carbon in the dead pool and high values in the live pool could indicate a treatment that was better at preserving carbon. Total carbon followed a similar trend as dead, carbon with Untreated (107.0 Mg/ha) containing the greatest median amount of total carbon, followed by Thin (88.0 Mg/ha) and Thin & Rx Burn (84.6 Mg/ha) (Figure 7c). For the total carbon pool, all treatments were statistically different in their effects on carbon, aside from Wildfire and Wildfire & Thin.

Overall, Untreated areas had the highest median values in the aboveground live, aboveground dead, and total carbon pools. We believe this demonstrates that untreated areas in the total carbon pool contained the largest amount of carbon per area prior to the fire, and therefore had an abundance of carbon to both lose (dead) and retain (live) following the wildfire event. Notably, the Wildfire area, an area that burned during the 2003 Overland Fire, had the largest discrepancy between its effect on the living and dead carbon pool, meaning that it retained higher amounts of living carbon and possessed lower amounts of dead carbon. This pattern may be an indicator of the effectiveness of frequent wildfires on carbon preservation in this system. Thin & Rx Burn also had a relatively high amount of live carbon compared to the other treatment types. Additionally, Thin, which was unique in its effect on carbon across pools, and Thin Twice had relatively low aboveground live carbon and a high level of aboveground dead carbon, indicating that thinning alone may not be an effective treatment. In general, our results highlighted that the sheer severity of the Cal-Wood fire likely rendered the carbon preservation efforts of the fuels reduction treatments less effective.

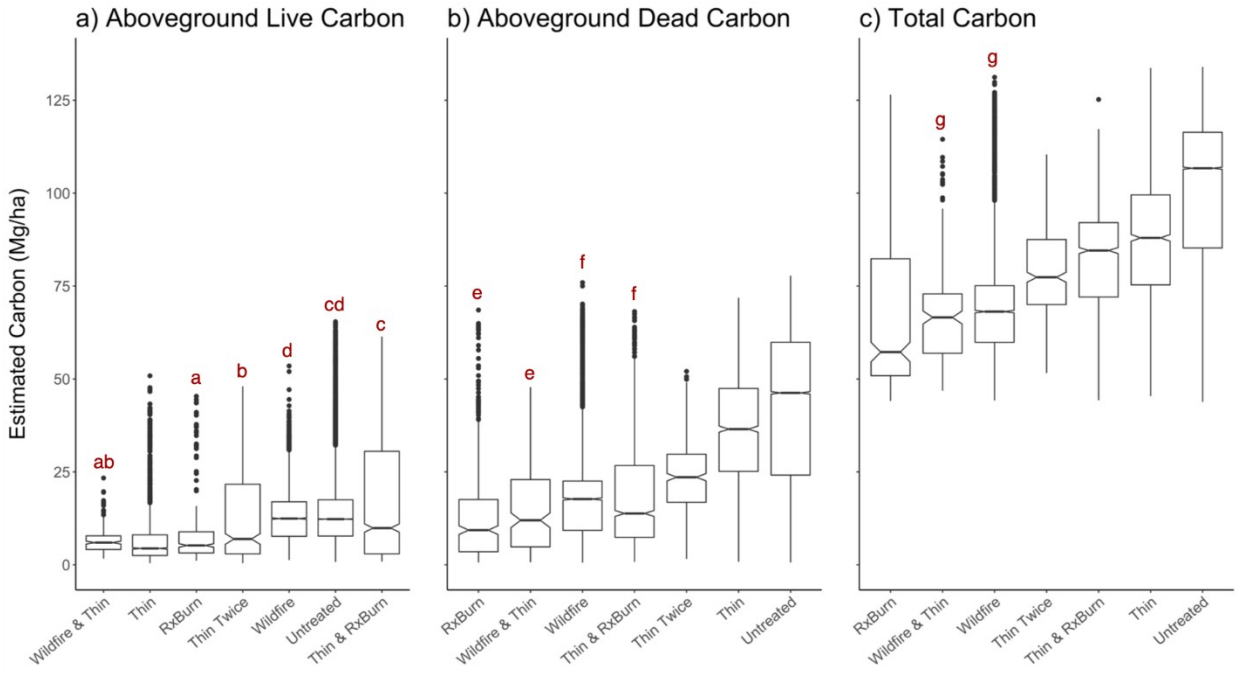


*Figure 7. a)* Aboveground live, *b)* Aboveground dead, and *c)* Total carbon (Mg/ha) for each treatment type. Treatment types are organized by the least (left) to greatest (right) mean carbon value. Letters above the box plot visualize the results from a pairwise Wilcoxon rank sum test using a threshold of $p < 0.01$. Matching letters indicate a lack of statistical difference for those treatment pairs, and no letter indicates treatments are different from all other treatments. Statistics are intended to compare treatments within a carbon pool and not across pools.

### *4.1.6 Study Area Landscape-Scale Carbon Distribution (Non-Treatment Models)*

In order to better understand carbon across the whole of the landscape, we present whole values in Gg of carbon, keeping in mind that treatment areas vary greatly in size across our study area. Some of the larger treatment areas in our study included Untreated areas which contained 79% of the total carbon in study area, followed by Wildfire areas (10% of the total carbon), Thin areas (5% of the total carbon), and Thin and Rx Burn areas (4% of the total carbon) (Figure 8). At the lower end of the treatment area, Wildfire & Thin, Rx Burn, and Thin Twice all contained less than 1% of the total carbon. As for live carbon, 76% is in Untreated, 14% in Wildfire, 5% in Thin & Rx Burn, 2% in Thin, and less than 2% in Wildfire & Thin, Rx Burn, and Thin Twice (Figure 8). For dead carbon, these values are 85% in Untreated, 7% in Wildfire, 5% in Thin, 2% in Thin & Rx Burn, and less than 1% in Wildfire & Thin, Rx Burn, and Thin Twice. Because Wildfire & Thin, Rx Burn, and Thin Twice contained less than 1% of the total carbon in the study area, this adds to uncertainties about conclusions drawn about the effect of these treatments on carbon preservation as smaller areas may not have experienced the fire uniformly.

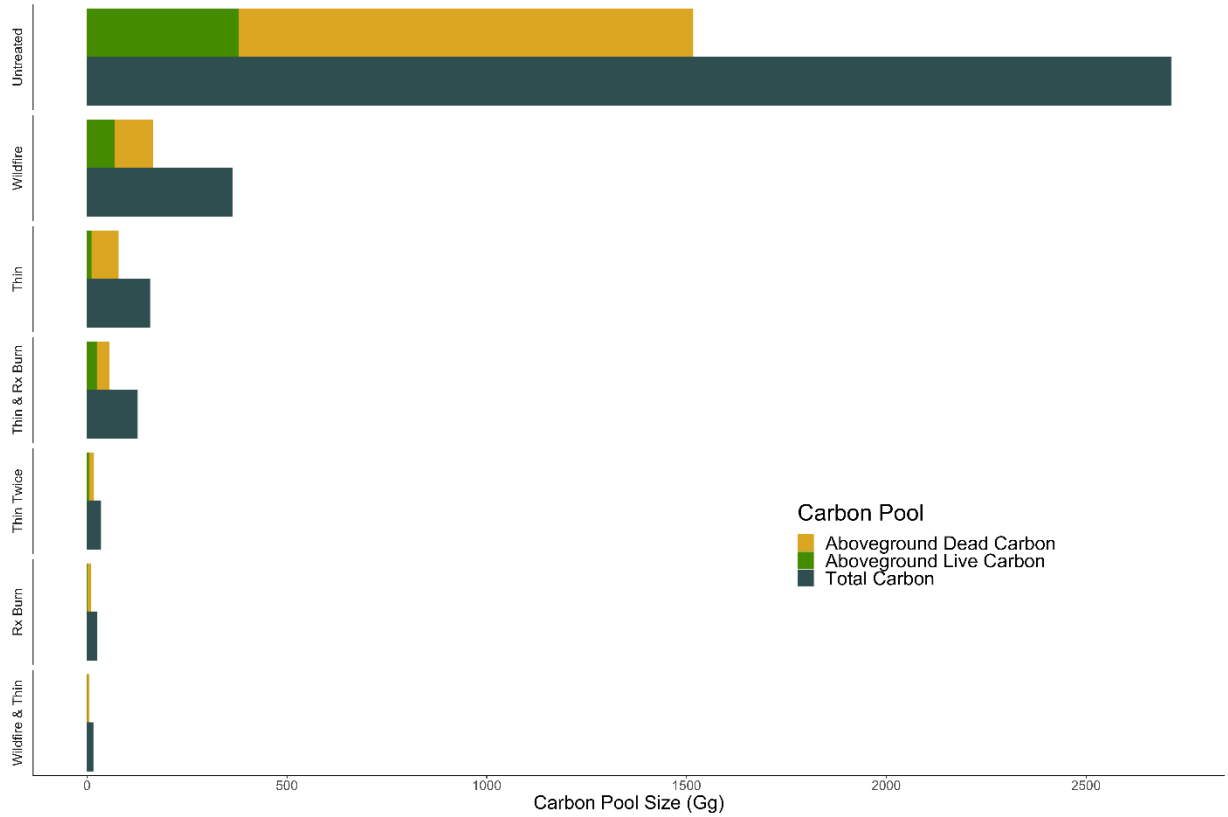


*Figure 8.* Carbon Pool Sizes (Gg) where the different colored bars represent the three carbon pools and their relationships to one another for each treatment type. Aboveground dead carbon depicted in yellow, aboveground live carbon in green, and total carbon in navy blue.

### *4.2 Caveats and Uncertainties*

We note that our study was observational and not experimental, meaning that the plots where our training data was collected might not have been able to effectively consider the landscape-scale variability of all variables such as elevation, aspect, or other environmental conditions that remote sensing is capable of capturing. For instance, the elevation only ranged from 1,790 to 2,120 m in our field plot data, whereas our study area varied from 1,500 to 2,830 m. These limitations in study design and data collection have the potential to influence our model outcomes. In addition, fires are complex, and the results of this study are only applicable to the Cal-Wood wildfire event on the CO Front Range.

Similarly, the treatment history of a landscape can also be complex. Our models were unable to capture the full complexity of treatment history within Heil Valley Ranch. Additionally, most of the field plots were located in areas with relatively low burn severity, which potentially skewed our data, especially for areas with small treatment coverage or untreated locations that experienced proportionately high burn severity. Thus, discretion must be used when considering our analysis of treatment effectiveness on carbon preservation. Furthermore, wildfire-impacted forests have the potential to be a carbon source for a prolonged amount of time due to trees dying for years after a wildfire. This prolonged carbon source could affect carbon pool estimations and the perceived effects of fuels reduction

treatments on carbon preservation within forested systems. Finally, our models do not suggest any relationship between carbon stocks and the predictor variables. Further investigation is needed to derive causal interactions between carbon and predictor variables.

### *4.3 Future Work*

Our methods can be implemented to develop post-fire carbon estimation models for other locations, and our analyses and conclusions can be used to inform future studies. Considering that our models did not capture the full complexity of the treatment history that occurred on this landscape, investigating the order, timing, and reoccurrence of treatments could provide additional information on their effectiveness. Additional future studies should train pre-fire remote sensing imagery with unburned and untreated sites to understand how treatments alone and both treatments and wildfire events redistribute carbon. Other forest types throughout CO should be considered by future studies to investigate if certain treatments are more effective at preserving carbon post-wildfire in one forest type over another. Finally, additional research to better understand the conditions when treatments become less effective would be highly valuable.

## 5. Conclusions

Community devastation, invasive species spread, loss of recreational opportunities, and weakened local economies due to high-severity wildfire events are the driving concerns behind the effective management of ponderosa pine forests throughout the CO Front Range. These concerns, combined with the threat of climate change exacerbating wildfire severity, frequency, and the length of the wildfire season, drive the evolution of proactive carbon focused forest management on the CO Front Range (Addington et al. 2018). The Cal-Wood fire provided us a unique opportunity to study the effectiveness of fuels treatments and the implications of wildfire on forest carbon stocks. This study investigated the feasibility of using remote sensing data paired with field-derived data to model post-fire forest carbon. We found that the RF models worked reasonably well to predict post-fire aboveground live, aboveground dead, standing, and total carbon pools. Overall, we believe the living carbon pool may have the most potential for monitoring post wildfire impacts on carbon preservation because it only considers carbon that survived the Cal-Wood fire event and is the model that performed best. Additionally, our models estimated that the aboveground dead carbon pool was approximately 2.5 times larger than the aboveground live carbon pool, highlighting the impact of the Cal-wood wildfire on carbon loss. Furthermore, untreated areas were shown to be the most effective at preserving carbon post-wildfire. However, we note that these untreated areas had greater amounts of pre-fire carbon than the treated areas, and therefore not only had more carbon to lose in the wildfire event, but also more carbon to retain following the wildfire. Although we did not explore it, greater amounts of pre-fire carbon in untreated areas may be associated with elevation and forest-type differences. The limitations presented here illustrated that more needs to be done to understand pre-fire carbon conditions on treated and untreated landscapes, and whether these treatments are the solution to forest carbon preservation in the face of wildfire. Nonetheless, the results of this study contribute to the efforts within the scientific community to compute post-fire forest carbon and can help land managers better understand carbon within their treated forests and the Cal-Wood fire.

## 6. Acknowledgments

The Boulder County Disasters team would like to thank our project partners, Nick Stremel and Dr. Brian Buma, for making this project possible. Additionally, we would like to thank our DEVELOP-affiliated advisors and mentors at the Fort Collins, CO node, Tony Vorster, Nick Young, Peter Engelstad, Paul Evangelista, Catherine Jarnevich, and Fellow, Scott Cunningham, for their support and guidance in the creation and completion of this project. We would also like to thank Jody Vogeler at CSU, Chris Wanner of City of Boulder, as well as Steve Murdock and Steve Germaine of Jefferson County for their contributions.

This material contains modified Copernicus Sentinel data (2020), processed by ESA.

Any opinions, findings, and conclusions or recommendations expressed in this material are those of the author(s) and do not necessarily reflect the views of the National Aeronautics and Space Administration.

This material is based upon work supported by NASA through contract NNL16AA05C.

## 7. Glossary

**Aboveground dead carbon** – carbon pool containing dead trees, dead seedlings, dead shrubs, and woody debris.
**Aboveground live carbon** – carbon pool containing living trees, living saplings, living shrubs, and grasses.
**BCPOS** – Boulder County Parks and Open Space
**CSU** – Colorado State University
**CTI** – compound topographic index
**DAAC** – Distributed Active Archive Center
**Earth observations** – Satellites and sensors that collect information about the Earth's physical, chemical, and biological systems over space and time
**EVT** – Existing vegetation type
**FCC** – forest canopy cover
**GEE** – Google Earth Engine
**LANDFIRE** – Landscape Fire and Resource Management Planning Tools
**LiDAR** – Light detection and ranging remote sensing method
**MSI** – Multi-spectral Instrument
**NED** – National Elevation Dataset
**OLI** – Operational Land Imager
**ORNL** – Oak Ridge National Laboratory
**Pairwise Wilcoxon rank sum test**- a nonparametric test that allows for comparisons between groups
**RF** – Random Forests, a machine learning algorithm that uses decision trees
**RMSE** – Root Mean Squared Error
**Rx Burn** – Prescribed burning, a practice of setting intentional surface-level fires.
**Soil carbon** – carbon pool containing organic (~0-10 cm) and mineral (~0-20 cm) soils.

**SRTM** – Shuttle Radar Topography Mission
**Standing carbon** – carbon pool containing living and dead trees.
**TOA** – Top of Atmosphere, in reference to satellite imagery reflectance
**Total carbon** – carbon pool containing aboveground live, aboveground dead, and soil carbon collectively.
**USGS**- United States Geological Survey
**VSURF** – Variable Selection Using Random Forests
**WUI** – Wildland Urban Interface

## 8. References


Abatzoglou, J. T., & Williams, A. P. (2016). Impact of anthropogenic climate change on wildfire across western US forests. *Proceedings of the National Academy of Sciences, 113*(42), 11770–11775. https://doi.org/10.1073/pnas.1607171113

Addington, R. N., Aplet, G. H., Battaglia, M. A., Briggs, J. S., Brown, P. M., Cheng, A. S., Dickinson, Y., Feinstein, J. A., Pelz, K. A., Regan, C. M., Thinnes, J., Truex, R., Fornwalt, P. J., Gannon, B., Julian, C. W., Underhill, J. L., & Wolk, B. (2018). Principles and practices for the restoration of ponderosa pine and dry mixed-conifer forests of the Colorado Front Range. *RMRS-GTR-373. Fort Collins, CO: U.S. Department of Agriculture, Forest Service, Rocky Mountain Research Station. 121*, *373*. https://doi.org/10.2737/RMRS-GTR-373

Agee, J. K., & Skinner, C. N. (2005). Basic principles of forest fuel reduction treatments. *Forest Ecology and Management*, *211*(1–2), 83–96. https://doi.org/10.1016/j.foreco.2005.01.034

Ali, S., & Salman, S. (2016). Landsat-8 (OLI) Classification Method Based on Tasseled Cap Transformation Features. *Al-Sadeq International Conference on Multidisciplinary in IT and Communication Science and Applications (AIC-MITCSA),* 1–5. http://dx.doi.org/10.1109/AIC-MITCSA.2016.7759914

Baig, M. H. A., Zhang, L., Shuai, T., & Tong, Q. (2014). Derivation of a tasselled cap transformation based on Landsat 8 at-satellite reflectance. *Remote Sensing Letters*, *5*(5), 423–431. https://doi.org/10.1080/2150704X.2014.915434

Biau, G., & Scornet, E. (2016). A random forest guided tour. *TEST, 25(2)*, 197–227. https://doi.org/10.1007/s11749-016-0481-7

Campbell, J. L., Harmon, M. E., & Mitchell, S. R. (2012). Can fuel reduction treatments really increase forest carbon storage in the western US by reducing future fire emissions? *Frontiers in Ecology and the Environment*, *10*(2), 83–90. https://doi.org/10.1890/110057

Dilling, L., Kelsey, K.C., Fernandez, D.P., Huang, Y.D., Milford, J.B., & Neff J.C. (2016). Managing carbon on federal public lands: Opportunities and challenges in Southwestern Colorado. *Environmental Management, (58)*, 283–296. https://doi.org/10.1007/s00267-016-0714-2

Evans, J., Oakleaf, J., Cushman, S., & Theobald D. (2014) An ArcGIS Toolbox for Surface Gradient and Geomorphometric Modeling, version 2.0-0. http://evansmurphy.wix.com/evansspatial.

Genuer, R., Poggi, J.-M., & Tuleau-Malot, C. (2010). Variable selection using random forests. *Pattern Recognition Letters*, *31*(14), 2225–2236. https://doi.org/10.1016/j.patrec.2010.03.014

Harrell, F. E., Lee, K. L., & Mark, D. B. (1996). Multivariable Prognostic Models: Issues in Developing Models, Evaluating Assumptions and Adequacy, and Measuring and Reducing Errors. *Statistics in Medicine*, *15*(4), 361–387. https://doi.org/10.1002/(SICI)1097-0258(19960229)15:4<361::AID-SIM168>3.0.CO;2-4

Kaufmann, M. R., Veblen T. T., & Romme W. H. (2006). Historical fire regimes in ponderosa pine forests of the Colorado Front Range, and recommendations for ecological restoration and fuels management. Front Range Fuels Treatment Partnership Roundtable, findings of the Ecology Workgroup. https://www.fs.usda.gov/treesearch/pubs/61131

Key, C. & Benson N. (2006). Landscape Assessment (LA) Sampling and Analysis Methods. *U.S. Department of Agriculture, Forest Service, Rocky Mountain Research Station. 164*, 1-55. https://doi.org/10.2737/RMRS-GTR-164

Liu, Z., Wimberly M. C., Lamsal, A., & Sohl, T. L. (2015). Climate change and wildfire risk in an expanding wildland–urban interface: a case study from the Colorado Front Range Corridor. *Landscape Ecology. 30*(10), 1943–1957. https://doi.org/10.1007/s10980-015-0222-4

Penman, J., Gytarsky, M., Hiraishi, T., Krug, T., Kruger, D., Pipatti, R., & Wagner, F. (2003). Good practice guidance for land use, land-use change and forestry. ISBN 4-88788-003-0

Rebain, S. A. (2010). The fire and fuels extension to the forest vegetation simulator: updated model documentation. In: Internal Report. US Department of Agriculture, Forest Service, Forest Management Service Center, Fort Collins, pp 1–397.

Shi, T., & Xu, H. (2019). Derivation of Tasseled Cap Transformation Coefficients for Sentinel-2 MSI At-Sensor Reflectance Data. *IEEE Journal of Selected Topics in Applied Earth Observations and Remote Sensing*, *12*(10), 4038–4048. https://doi.org/10.1109/JSTARS.2019.2938388

Swayze, N., Tsz Hin Choi, C., Knowlton, G., & Klisauskaite, J. (2021). Colorado Front Range Disasters. Understanding the Impact of Forest Management on the Cameron Peak and CalWood Fire [Unpublished manuscript]. CO Node, NASA DEVELOP.

Tsitsi, B. (2016). Remote sensing of aboveground forest biomass: A review. *Tropical Ecology, 57*(2), 125-132. ISSN 0564-3295

Vashum, K. T., & Jayakumar, S. (2012). Methods to estimate above-ground biomass and carbon stock in natural forests - a review. *Journal of Ecosystem & Ecography, 2*(4), 116. https://doi.org/10.4172/2157-7625.1000116

Veblen, T., & Lorenz, D. (1991). The Colorado Front Range - A Century of Ecological Change. 1st ed. Salt Lake City, Utah: University of Utah Press.

Westerling, A. L. (2016). Increasing western US forest wildfire activity: Sensitivity to changes in the timing of spring. *Philosophical Transactions of the Royal Society B, 371*(1696), 20150178. http://doi.org/10.1098/rstb.2015.0178

# 9. Appendices

## Appendix A: Predictor Variables

**Table A1.**
*Remotely sensed and ancillary data products imported into R for use as predictor variables.*

| Predictor Variable | Source | Dates |
|---|---|---|
| Elevation, slope, aspect, northness, eastness, curvature, profile curvature, plan curvature, heat load index, roughness, CTI | SRTM- USGS NED | February 11$^{th}$ – 22$^{nd}$, 2000 |
| Existing Vegetation Type (EVT), Forest Canopy Cover (FCC) | LANDFIRE | EVT (2016); FCC (2020) |
| Tasseled cap greenness, brightness, wetness, and difference | Landsat 8 OLI tier 1 TOA; Sentinel-2 MSI Level-C1 | Pre-Fire- October 6$^{th}$, 2020; Spring- June 12$^{th}$, 2021; Summer- September 7$^{th}$, 2021; Fall- November 2$^{nd}$, 2020 Fire- (Spring – Pre-Fire) Regrowth- (Summer – Spring) |
| Burn severity | CSU Product | September 1$^{st}$ – December 31$^{st}$, 2020 |
| Height metrics- skewness, standard deviation, kurtosis, max, height variation coefficient (CV), 99$^{th}$ percentile of height (P99), 95$^{th}$ percentile of height (P95), 75$^{th}$ percentile of height (P75), 50$^{th}$ percentile of height, 25$^{th}$ percentile of height (P25) Canopy metrics- average height, maximum height, standard deviation | Vogeler Research Lab, CSU LiDAR data | 2013 |
| Soil percent clay, silt, sand, organic matter and pH (0-20 cm) | NRCS Web Soil Survey | September 2$^{nd}$, 2021 |
| Soil carbon (0-20 cm) | ORNL DAAC | 1970 – 1993 |
| Treatment type, age, and presence | Collaborative Treatment Database | 2003 – 2021 |

## Appendix B: Tasseled Cap Transformation Coefficients

**Table B1.**
*Coefficients for Tasseled Cap Transformations for Landsat 8 OLI tier 1 TOA reflectance imagery (Baig et al., 2014).*

| Index | Band 2 (Blue) | Band 3 (Green) | Band 4 (Red) | Band 5 (NIR) | Band 6 (SWIR1) | Band 7 (SWIR2) |
|---|---|---|---|---|---|---|
| Brightness | 0.3029 | 0.2786 | 0.4733 | 0.5599 | 0.508 | 0.1872 |
| Greenness | -0.2941 | -0.243 | -0.5424 | 0.7276 | 0.0713 | -0.1608 |
| Wetness | 0.1511 | 0.1973 | 0.3283 | 0.3407 | -0.7117 | -0.4559 |

**Table B2.**
*Coefficients for Tasseled Cap Transformations for Sentinel-2 MSI reflectance imagery (Shi & Xu, 2019).*

| Index | Band 2 (Blue) | Band 3 (Green) | Band 4 (Red) | Band 8 (NIR) | Band 11 (SWIR1) | Band 12 (SWIR2) |
|---|---|---|---|---|---|---|
| Brightness | 0.3510 | 0.3813 | 0.3437 | 0.7196 | 0.2396 | 0.1949 |
| Greenness | -0.3599 | -0.3533 | -0.4734 | 0.6633 | 0.0087 | -0.2856 |
| Wetness | 0.2578 | 0.2305 | 0.0883 | 0.1071 | -0.7611 | -0.5308 |

## Appendix C: Treatment Models

**Table C1.**
List of best models and their performance ratings for each Treatment carbon pool model.

| Carbon Pool | $R^2$ | RMSE (Mg/ha) | %RMSE | Included Treatment Variables (Y/N) | Predictor Variables (in order of importance) |
|---|---|---|---|---|---|
| Aboveground Live Carbon | 0.76 | 10.8 | 77.8% | N | • Post-fire tasseled cap greenness (Fall 2020)<br>• Burn severity<br>• Regrowth-related difference in tasseled cap brightness |
| Standing Carbon | 0.44 | 19.5 | 54.6% | N | • Forest Canopy cover<br>• Average LiDAR canopy height<br>• Pre-fire tasseled cap wetness |
| Aboveground Dead Carbon | 0.42 | 21.2 | 82.5% | Y | • Post-fire tasseled cap greenness (Spring 2020)<br>• Fire-related difference in tasseled cap greenness<br>• Regrowth-related difference in tasseled cap |
| Total Carbon | 0.40 | 23.7 | 28.0% | Y | • Average LiDAR canopy height<br>• Post-fire tasseled cap brightness (Spring 2021)<br>• Post-fire tasseled cap greenness (Fall 2020) |
| Soil Carbon | 0.20 | 12.5 | 27.8% | Y | • Treatment type<br>• Post-fire tasseled cap wetness (Fall 2020) |